International Journal of Steel Structures (2020) 20(6):1882–1890
https://doi.org/10.1007/s13296-020-00375-9

Online ISSN 2093-6311
Print ISSN 1598-2351

Applicability Evaluation of Clean Laser System in Surface Preparation on Steel

Jin-Eun Park[1] · Kab-Soo Kyung[2] · Myeong-Gi Moon[2] · Ik-Sang Yun[3] · Myung-Jin Eum[4]

Received: 6 February 2020 / Accepted: 5 July 2020 / Published online: 17 July 2020

Abstract
Surface preparation is a critical process in the re-painting of steel bridges wherein the grinding or blasting method has been widely used to remove coating and rust off steel surfaces. However, these methods struggle with rust removal in narrow areas, causing environmental problems such as dust scattering, and noise. In order to solve these problems, surface preparation, using a laser, has been researched and developed. In this study, we investigated the applicability of the clean laser system to the surface preparation of steel, experimentally, and analytically. The coating and rust removal experiments, using the clean laser system were performed with two types of specimens, both employing different coating systems. Furthermore, the coating thickness, surface observation using a microscope, and adhesion test were investigated during the tests. Subsequently, the thermal finite element analysis was performed under the same conditions as that of the experiments. It was revealed that the optimal condition for coating and rust removal was determined by the laser power, pulse width, scan width, and scan speed.

Keywords Surface preparation · Clean laser · Repainting · Coating · Rust

1 Introduction

Steel bridges are subjected to corrosion and deterioration damage, under various environmental conditions, as the number of service years increases. These damages not only reduce the load-carrying capacity and durability of the structure but also hinder the visual aesthetics of the structure (Mun et al. 2017; Kim et al. 2018). The coating method is widely employed as an anti-corrosion method to steel structures, and the quality of surface preparation at the time of repainting is known to have a significant influence on the durability after repainting (Lee et al. 2015).

✉ Kab-Soo Kyung
kyungks@kmou.ac.kr

[1] Leaders in Industry-University Cooperation+, Korea Maritime and Ocean University, Taejong-ro, Yeongdo-gu,, Busan 49112, Korea

[2] Department of Civil Engineering, Korea Maritime and Ocean University, Taejong-ro, Yeongdo-gu, Busan 49112, Korea

[3] Mechanical Safety Technology Center, Korea Testing Laboratory, Chungui-ro, Jinju, Gyeongsangnam-do 52852, Korea

[4] Micro Imaging, Kwanggyo-ro, Suwon, Gyeonggi-do 16229, Korea

Several surface preparation methods such as chemical methods, grinding, and blasting methods (spray sand, plastic grain, etc.) are used to remove rust and paint from the steel surface at the time of repainting. However, these methods are subject to problems such as the scattering of dust containing harmful substances, an increase in industrial waste, and early deterioration due to noise and failure of surface preparation, among others. In order to solve these problems, a cleaning method that employs a laser of high energy density that instantly sublimates and evaporates the surface material to remove the coating and rust has attracted the attention of developed countries.

Laser cleaning is a technology that has been developed in Germany and is being introduced into the aviation, automotive, and medical device sectors, wherein environmental regulations are strict. Additionally, as a non-contact dry process, secondary wastes are not produced owing to the absence of the use of chemicals, and abrasives. The most representative laser cleaning systems are R&D and commercialization of Clean Laser in Germany, P-Laser in Belgium, Perfect Laser in China, Laser Photonics in the US, and Cool Laser in Japan.

Laser cleaning has a high initial cost as compared to other methods and requires significant repetitive work for application to bridges owing to the narrow laser scan width.

Additionally, the durability of the laser gun is low, and the use of the laser gun for prolonged periods is challenging. It is also necessary to install a dust collector for fly ash when removing the coating and rust by means of laser cleaning. Moreover, in order to apply the clean laser system to surface preparation, detailed specifications such as the laser type, power, pulse width, scan width, and speed of the laser system should be determined according to the coating system.

In Korea, limited research surrounding the clean laser system has been performed. Furthermore, only relevant patents are studied, and there exists no practical application for these patents. In this study, we investigated the applicability of a clean laser system to the surface preparation of steel, experimentally. The coating and rust removal tests, using the clean laser system, were performed with two types of specimens, employing different 3 coating systems. Moreover, the coating thickness, surface observation using a microscope, and adhesion were investigated during the tests.

2 Experimental Procedures

2.1 Outline of Laser System

Lasers are classified into pulse lasers, which operate in a way wherein all of its energy is outputted in a single pulse, and CW lasers, which continuously emit laser light, and are used for all steel surface preparation (Jujii et al. 2018). The laser system applied in this study is the nLIGHT CFL-4000, which employs the CW laser method.

For the test using the clean laser system, an experimental environment consisting of a laser control system and laser scanning device was prepared, as shown in Fig. 1. The laser scan range was 500 mm × 500 mm, with a vertical movement of up to 100 mm, and a laser scan rate of up to 200 mm/s. Through the control system, the laser power, pulse width, scanning width, and scanning speed can be constantly controlled.

2.2 Specimen Configuration

The test specimens were applied with heavy-duty coating under general environmental conditions (Urethane finish type) and heavy-duty coating in special environmental conditions (PVDF finish type), as shown in Fig. 2. The test specimens were manufactured by referring to the standard specification of steel structure construction in Korea, and are shown in Table 1. Additionally, to produce the corrosion test specimen, X-cut scratching were put on the steel surface. After then, spraying 10% NaCl solution for 30 min and drying at the atmosphere for 30 min were repeated for a month.

2.3 Test Matrix

The coating removal tests using the clean laser system were based on laser power, pulse width, scan width, and scan speed. Table 2 shows the testing parameters.

The relationship between the laser power and pulse width was investigated when the laser scan width was 35 mm. After then, the relationship between the laser pulse width and scan speed was investigated when the laser scan width was 70 mm. In the case of the corrosion test specimens, the test was conducted using a laser width of 70 mm, a laser power of 1000 W, a pulse width of 5 kHz, and a laser speed of 5 mm/s.

Furthermore, test specimens were labeled A for general environmental coating and B for special environmental coating. Furthermore, specimens were then named by their parameters. For example, the test specimen A-500-5-10-35 was subjected to a laser of power 500 W, a pulse width of 5 kHz, a laser scan speed of 10 mm/s, and a laser scan width of 35 mm.

2.4 Measuring Equipment

In order to investigate the removal efficiency and performance of coating removal using the clean laser system, the coating

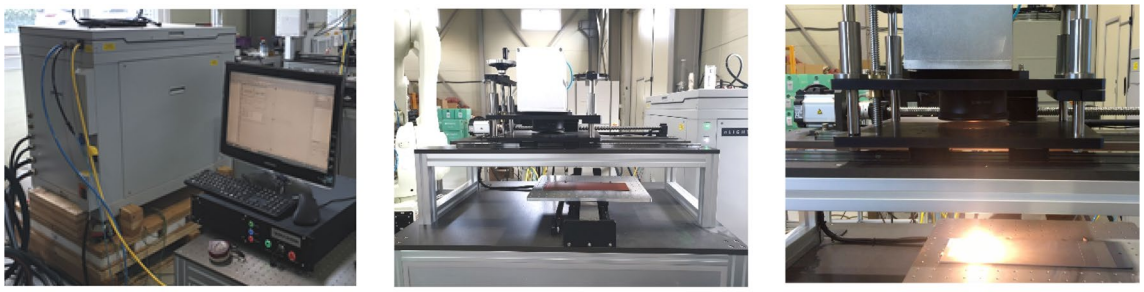

(a) Control system **(b)** Laser scan device **(c)** Test setup

Fig. 1 Clean laser equipment

Fig. 2 Specimen configuration

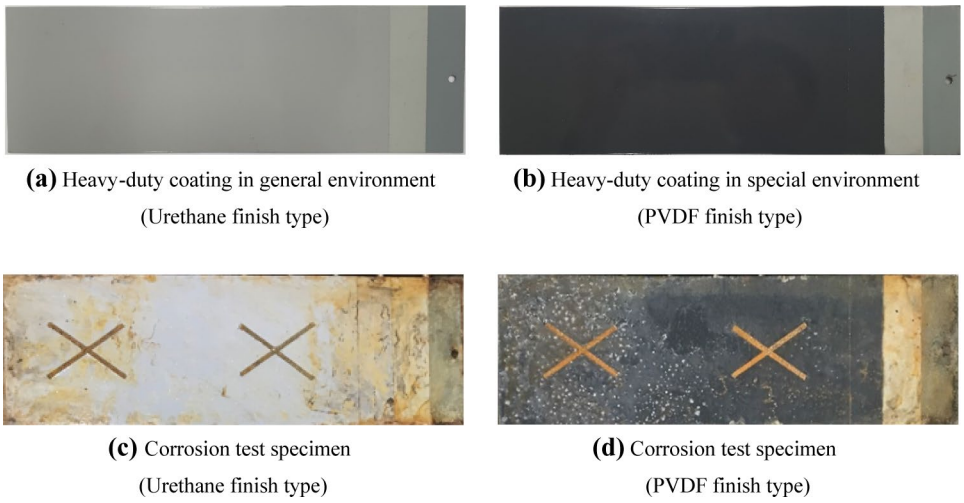

(a) Heavy-duty coating in general environment (Urethane finish type)

(b) Heavy-duty coating in special environment (PVDF finish type)

(c) Corrosion test specimen (Urethane finish type)

(d) Corrosion test specimen (PVDF finish type)

Table 1 Manufacturing conditions for heavy-duty coating specimens

Process	General environmental		Special environmental	
	Paint type	Thickness (μm)	Paint type	Thickness (μm)
First surface treatment	SSPC SP10	–	SSPC SP10	–
Shop Primer	Inorganic zinc powder shop primer	20	Inorganic zinc powder shop primer	20
Second surface treatment	SSPC SP10	–	SSPC SP10	–
1st layer	Inorganic zinc powder paint	75	Inorganic zinc powder paint	75
2nd layer	Mist Coat	–	Mist Coat	–
3rd layer	High solid epoxy type paint	80	High solid epoxy type paint	100
4th layer	Urethane type paint	30	Poly Vinylidene Fluoride type paint	25
5th layer	Urethane type paint	30	Poly Vinylidene Fluoride type paint	25
Total		215		225

Table 2 Testing parameters

Laser power (W)	Laser pulse width (kHz)	Laser scan speed (mm/s)	Laser scan width (mm)
500 1000 1500 2000	5 10	5 10	35 70

thickness and surface observation using a microscope were measured and conducted during the test, respectively. Additionally, in order to investigate the applicability of repainting after surface preparation using the clean laser system, the adhesion test was performed after the coating was removed, and the shop primer coating was applied.

3 Test Results

3.1 Measurement Result of Coating Thickness

In this section, the change in coating thickness according to the laser power, pulse width, scan width, and scan speed is summarized using the below-described test. The coating thickness was measured during the test, and the average value reported from 5 different sections of the specimen was used as the test result.

Figure 3 shows the relationship between the change in coating thickness, laser power (500, 1000 W), and laser pulse width (5, 10 kHz) when the laser width was 35 mm. It was found that the rate of coating removal increased when the laser power and pulse width increased. The laser pulse width has more influence on coating removal than the laser power. Additionally, for the B-500-5-5-35 specimen, the same experiment was repeated more than ten times; however, the laser did not reach the shop primer layer. For the B-2000-10-5-35 specimen, the entire coating

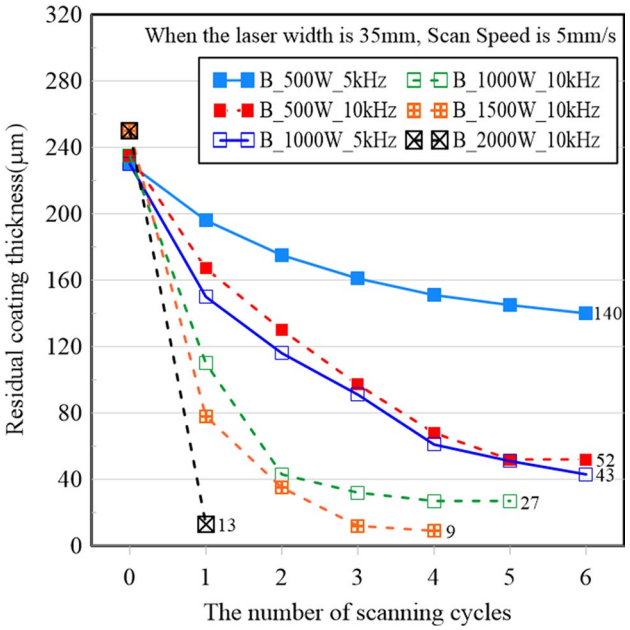

Fig. 3 Changes of coating thickness by the laser power and the pulse width when the laser width is 35 mm

was removed at the same time. However, thermal deformation and melting of the base metal were observed in the specimen.

Figure 4 shows the relationship between the change in coating thickness, laser pulse width (5, 10 kHz) and the laser scan width (35, 70 mm) when the laser power was 1000 W. It can be seen that rate of coating removal increased when the laser scan width decreased. This phenomenon is attributed to the fact that energy is dispersed as the laser scan width increases. Additionally, when the laser width was 35 mm, the rate of coating removal tended to increase as the pulse width increased. However, when the laser width was 70 mm, the rate of coating removal did not increase according to the laser pulse width, significantly. The relationship between the change in coating thickness and laser scan width for specimens under general environmental conditions is the same as that of the specimen under special environmental conditions, and the rate of coating removal increased when the laser scan width decreased.

Figure 5 shows the relationship between the change in coating thickness, laser pulse width (5, 10 kHz), and laser scan speed (5, 10 mm/s) when the laser pulse scan width was 70 mm. It was found that the rate of coating removal increased when the laser scan speed decreased. Moreover, these results were similar regardless of the coating system.

3.2 Prediction Model for Change in Coating Thickness for the Clean Laser System

The relationship between the change in coating thickness and the parameters (laser power, laser scan width, and scan speed) revealed that the rate of coating removal increased when the laser power was increased, and laser scan width and scan speed were decreased. Based on these results, the prediction model for the change in coating thickness for the clean laser system is suggested by introducing a correlation coefficient. The correlation coefficients were calculated by

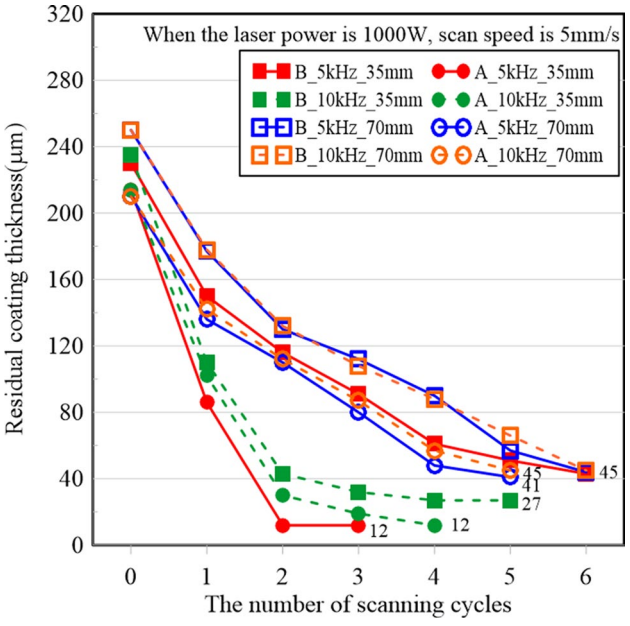

Fig. 4 Changes of coating thickness by the laser pulse width and scan width when the laser power is 1000 W

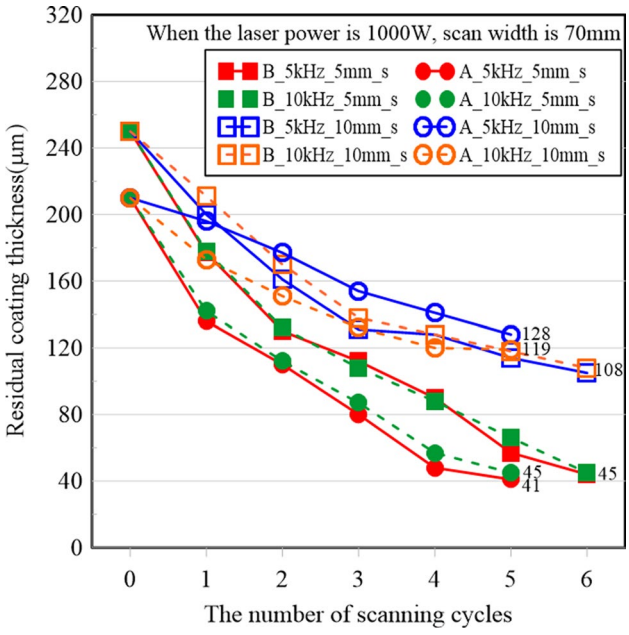

Fig. 5 Changes of coating thickness by the laser pulse width and scan speed when the laser power is 1000 W

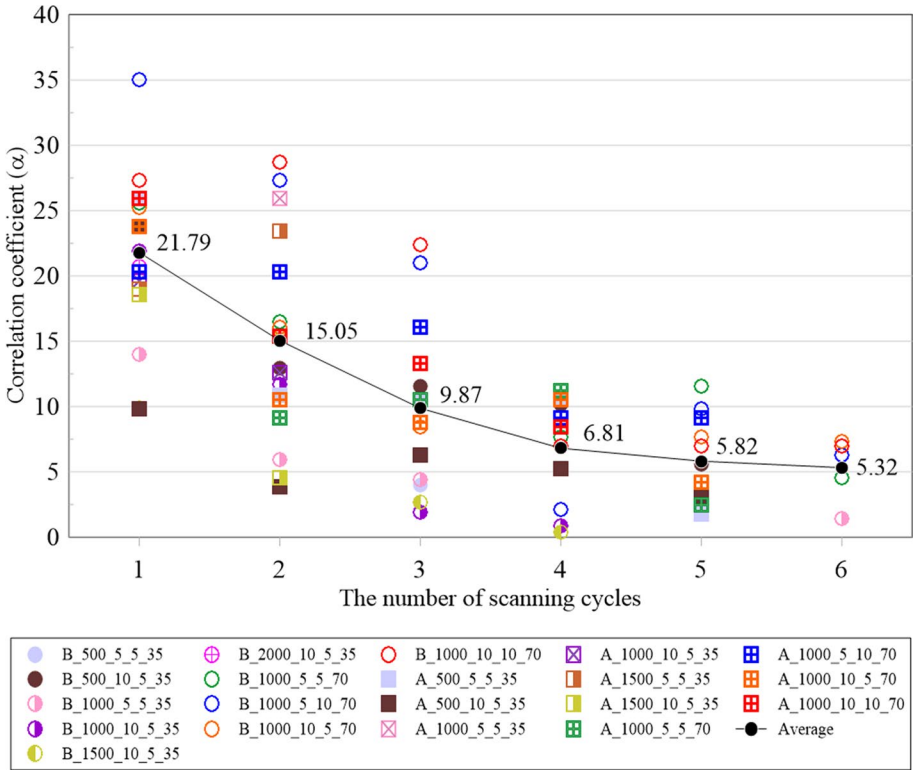

Fig. 6 Relationship between correlation coefficient and the number of scanning cycles

Eq. (1). Figure 6 shows the relationship between the correlation coefficient and the number of scanning cycles in order to calculate removal amount of coating thickness. From the prediction model, it can be inferred that removal amount of coating thickness can be controlled by means of the laser power, scan width, and scan speed.

$$\text{Correlation coefficient } (\alpha) = \frac{\text{Removal amount of coating thickness at each specimen}}{\left[\text{Laser power}/(\text{scanning width} \times \text{scanning speed})\right]} \quad (1)$$

3.3 Surface Observation Using Microscope in the Corroded Specimen

The optimal conditions for coating and rust removal were determined by means of the results of coating thickness and surface roughness measurements when the laser power was 1000 W, the laser pulse width was 5 kHz, the laser scan width was 70 mm, and the laser scan speed was 5 mm/s (Park et al. 2019). Based on these conditions, the coating and rust removal test using the clean laser system was performed, and the surface observation using a microscope was investigated.

The laser scans were repeated five times for coatings under general environmental conditions and six times for coatings under special environmental conditions, and the results are shown in Fig. 7. Rust was removed immediately at the same time, and some soot remained on the surfaces. However, it is indicated that rust removal is possible using the clean laser system before and after the test.

3.4 Adhesion Test Results

For the adhesion test, the cross-cut tape test was applied by referring to the Maintenance manual for corrosion prevention of steel bridges in Korea (2003) and ASTM D3359-97. The adhesion test was performed on the specimens satisfying the standard repainting range during surface roughness measurements. An example of the results is shown in Fig. 8. As a result of the adhesion test, all the specimens were evaluated as Grade 3B. Grade 3B represents the status in which the area affected ranges between 5 and 15% of the lattice (ASTM D3359-97).

4 Overview of Finite Element Analysis

4.1 General Introduction for Structural Analysis

In order to simulate the structural behavior under the operation of the laser of the clean laser system by means of the analytical method, the light energy from the clean laser is converted into thermal energy. This method also requires information concerning material properties that change with temperature. In this study, the thermal analysis of uncoated general structural steel (SS235) was carried out without considering the coating in the structural analysis.

The material model presented in Eurocode 3 (1995) was used for general structural steel. For accurate analysis, the true stress–strain relationship was used, considering the cross-sectional change due to deformation.

Eurocode 3 presents the thermal and mechanical properties of general structural steels. The thermal properties such as thermal conductivity, specific heat, and elongation at high temperatures of general structural steels are shown by the general equation, as shown in Table 3. The coefficient of thermal expansion is not presented directly. However, it is obtained by calculation because it implies the tangential slope of the elongation curve.

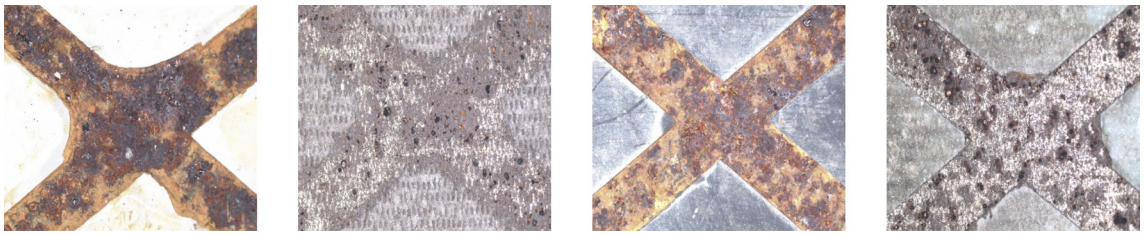

(a) Heavy-duty coating in general environments **(b)** Heavy-duty coating in special environments

Fig. 7 Changes in rust removal with repeated laser scan in the tests

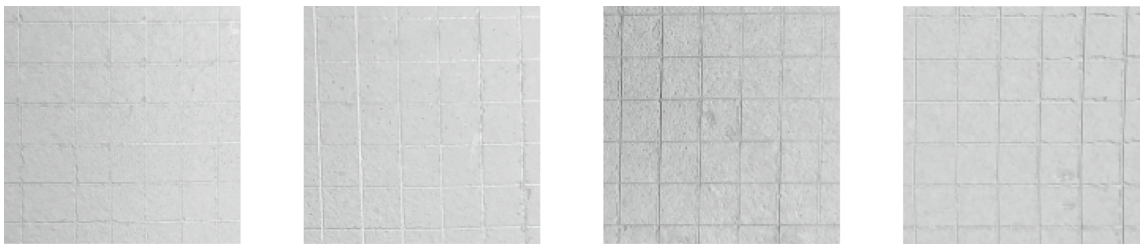

(a) A-1000-5-5-70 **(b)** A-1000-10-5-70 **(c)** B-1000-5-5-70 **(d)** B-1000-10-5-70

Fig. 8 Examples of adhesion test results

Table 3 Thermal properties of general steels (Eurocode 3)

Properties	Equations	Steel temperature (θ_a)
Density (kg/m^3)	$\rho = 7850$	–
Conductivity (W/m °C)	$\lambda_s = 54 - 3.33 \times 10^{-2}\theta_a$	$20 \le \theta_a < 800$
	$\lambda_s = 27.3$	$800 \le \theta_a \le 1200$
Specific heat (J/kg °C)	$C_a = 425 + 7.73 \times 10^{-1}\theta_a - 1.69 \times 10^{-3}\theta_a^2 + 2.22 \times 10^{-6}\theta_a^3$	$20 \le \theta_a < 600$
	$C_a = 666 + \frac{13002}{738-\theta_a}$	$600 \le \theta_a < 735$
	$C_a = 545 + \frac{17820}{\theta_a-731}$	$735 \le \theta_a < 900$
	$C_a = 650$	$900 \le \theta_a \le 1200$
Elongation	$\Delta l/l = 1.2 \times 10^{-5}\theta_a + 0.4 \times 10^{-8}\theta_a^2 - 2.416 \times 10^{-4}$	$20 \le \theta_a < 750$
	$\Delta l/l = 1.1 \times 10^{-2}$	$750 \le \theta_a \le 860$
	$\Delta l/l = 2 \times 10^{-5}\theta_a - 6.2 \times 10^{-3}$	$860 \le \theta_a \le 1200$

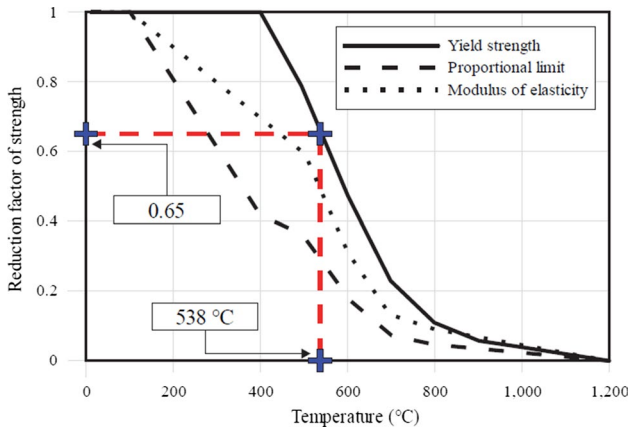

Fig. 9 Reduction factor of strength for general structural steels at high temperature—Eurocode 3

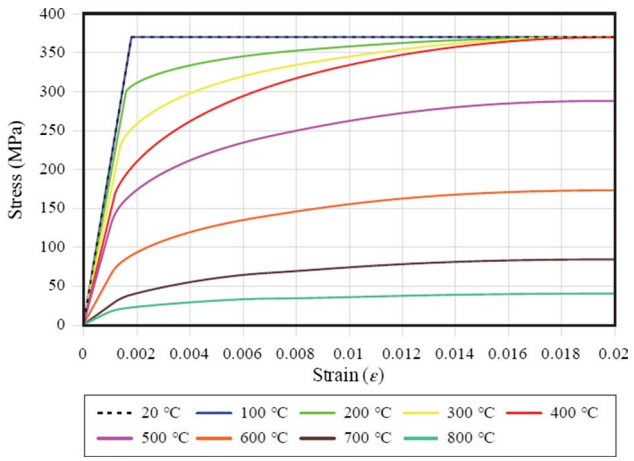

Fig. 10 Relationship between stress and strain of general structural steel at high temperature

The reduction factor applied to the strength of general structural steels at high temperatures is shown in Fig. 9. The graph can be applied to all structural steels with a room temperature yield strength of less than 448 MPa. As shown in Fig. 9, the yield strength of general structural steel starts to drop sharply after 400 °C and it is reduced to less than 50% of the yield strength after 600 °C.

Eurocode 3 (1995) provides a detailed model of the stress–strain relationship for carbon steels. Figure 10 shows the relationship between stress and strain of general structural steel at high temperatures. In this figure, as the temperature increases, the nonlinearity also increases due to the rapid decrease of the proportional limit, and the yield strength drops rapidly after 400 °C.

4.2 Analysis Method

In this study, the ABAQUS program was applied to evaluate the thermal distribution of the clean laser system. The program includes a reliable thermal conduction analysis, which allows nonlinear thermal conduction analysis of assumed thermal energy conditions.

The transient heat transfer analysis was performed to predict the nonlinear temperature distribution of the structure considering thermal conditions and time history. The element was applied using DC3D8, a three-dimensional eight-node solid element. The governing heat transfer equations, calculated in the program, are based on the energy equilibrium theory of Green and Naghdi (ABAQUS Manual 2016), assuming steel temperature changes due to conduction, convection, and radiation. The convective heat transfer coefficient, the emissivity, and the Stefan–Boltzmann constant are 25 W/m^2 K, 0.7 and 5.67×10^{-8} W/m^2 K^4, respectively. These values are recommended in Eurocode 3.

5 Finite Analysis Model and Results

The analysis model was based on the test conducted in Sects. 2 and 3, and the analysis was performed based on a laser power of 100 W and a laser scan speed of 5 mm/s. The dimension of the specimen used in the test was 100 mm × 300 mm, and a thickness of 3 mm, as shown in Fig. 2. The heat energy was calculated by determining the power, scan width and scan speed of the clean laser as surface heat flux (Mo et al. 2006), as shown in Eq. 2.

$$\text{Heat flux} = \frac{\text{Laser power}}{\text{Laser scanning width} \times \text{Laser scanning speed}} \quad (2)$$

Figure 11 shows the result of the heat transfer analysis when the laser scan width is 35 mm. When the laser scan width is 35 mm, the surface temperature begins to change at approximately 400 °C within 1 s of the start of the scan, and changes to 730 °C in 7 s and 680 °C in 14 s. The laser scan begins at 60 s (46 s after the end of the laser scan), and the temperature is reduced to 170 °C. Although the surface temperature exceeds 700 °C quickly, the temperature decreases rapidly after the laser scan.

Figure 12 shows the result of the heat transfer analysis when the laser scan width is 70 mm. When the laser scan width is 70 mm, the surface temperature begins to change at approximately 210 °C within 1 s of the start of the scan, and changes to 430 °C in 7 s and 390 °C in 14 s. The laser scan begins at 60 s (46 s after the end of the laser scan), and the temperature is reduced to 155 °C. Compared to the laser scan width of 35 mm, the surface temperature was not

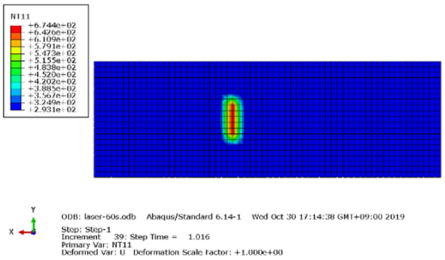

(a) 1 second after laser scan
(max. surface temperature : 400˚C)

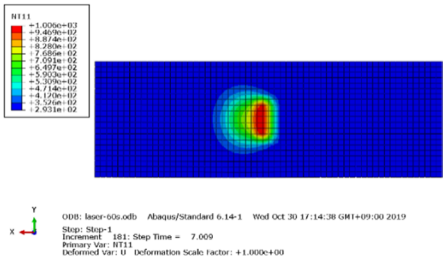

(b) 7 second after laser scan
(max. surface temperature : 730˚C)

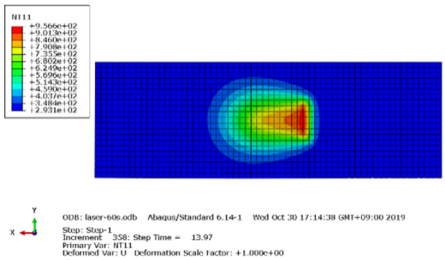

(c) 14 second after laser scan
(max. surface temperature : 680˚C)

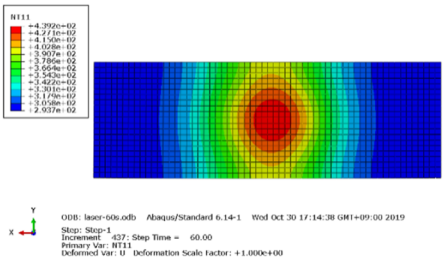

(d) 60 second after laser scan
(max. surface temperature : 170˚C)

Fig. 11 Analysis results when the laser scan width is 35 mm

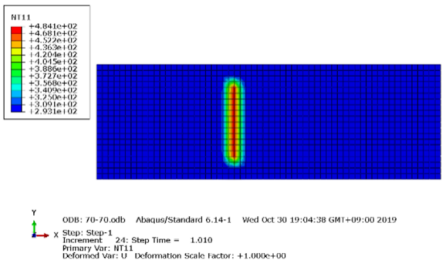

(a) 1 second after laser scan
(max. surface temperature : 210˚C)

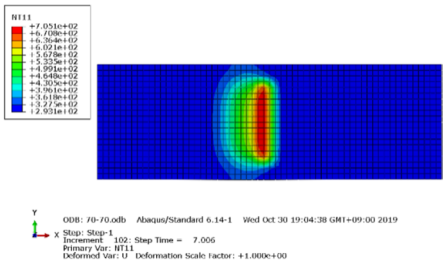

(b) 7 second after laser scan
(max. surface temperature : 430˚C)

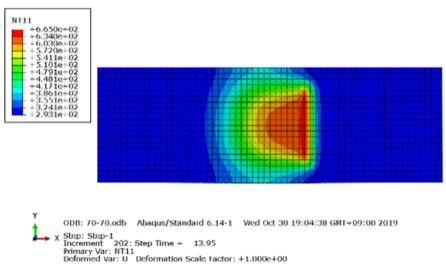

(c) 14 second after laser scan
(max. surface temperature : 390˚C)

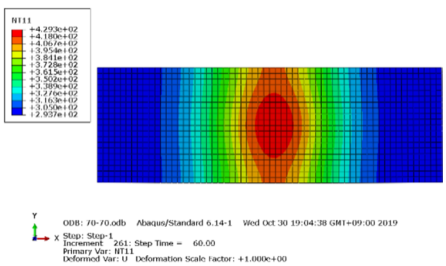

(d) 60 second after laser scan
(max. surface temperature : 155˚C)

Fig. 12 Analysis results when the laser scan width is 70 mm

high, and the surface temperature decreased rapidly after the laser scan.

The laser cleaning system concentrates high energy in small areas, allowing for local surface treatment. Additionally, due to the minimal heat-affected zone, the dimensional deformation due to heat treatment was hardly observed. When the heat source is removed after the laser scan, a rapid temperature gradient is generated due to the thermal conduction of the material, which causes self-quenching (Hwang et al. 2011).

6 Conclusions

In this study, we investigated the applicability of the clean laser system to the surface preparation of steel, experimentally and analytically. The coating and rust removal experiments using the clean laser system were performed with two types of specimens, employing different coating systems. The coating thickness, surface observation using a microscope, and adhesion were investigated during the experiments. Then, the thermal finite element analysis was performed under the same conditions as that of the tests. The conclusions of this study are summarized follows.

(1) The relationship between the coating thickness and parameters (laser power, scan width, and scan speed) revealed that the rate of coating removal increased when the laser power increased, and the laser scan width and scan speed decreased. Based on these results, the prediction model concerning the removal amount of coating thickness for the clean laser system is suggested by introducing the correlation coefficient.
(2) In order to simulate the thermal behavior under the operation of the clean laser system, the thermal analysis of uncoated, general structural steel was carried out without considering the coating in the structural analysis. The surface temperature exceeded 700 °C quickly, however, the temperature decreased rapidly after the laser scan. These temperature gradients on the surface can cause a self-quenching effect

Acknowledgements This research was carried out from the research support of the Ministry of Land, Infrastructure and Transport Construction Technology Research Project (18CTP-C143604-01).

References

Dassault Systèmes Simulia Corp. (2016). *ABAQUS theory manual, Ver. 6.12*. Providence: DSS.

European Committee for Standardization. (1995). *Eurocode 3: Design of steel structures, part 1.2: General rule -structural fire design* (ENV 1993-1-2: 1995), Belgium.

Hwang, H. T., Choi, H. W., & Kim, J. D. (2011). A study on laser surface treatment characteristics of high carbon steel (HP4MA) for injection mold. *Korean Society of Manufacturing Technology, KSMTE, 20*(5), 646–652. **(in Korean)**.

Jujii, K., Kitane, Y., & Nakano, T. (2018). Applicability of laser cleaning for surface preparation of steel. *Bridge and Foundation Engineering, Kensetutosyo, 52*(10), 31–34. **(in Japanese)**.

Kim, H. S., Shin, C. H., Dao, D. K., Jeong, Y. S., & Kim, I. T. (2018). Evaluation on residual compressive strength of welded circular tubular members with locally corroded ends. *Journal of Korean Society of Steel Construction, KSSC, 30*(3), 145–152. **(in Korean)**.

Lee, C. Y., Jung, M., Park, J. W., Lee, I. Y., & Jang, S. D. (2015). Case study on maintenance coatings for steel arch bridge considering corrosion environment of bridge members. *Magazine of the Korean Society of Steel Construction, KSSC, 27*(2), 29–33. **(in Korean)**.

Ministry of Construction & Transportation. (2003). *Maintenance Manual for Corrosion Prevention of Steel Bridges* (pp. 87–89). Sejong: MOCT. **(in Korean)**.

Mo, Y. W., Yoo, Y. T., Shin, B. H., & Shin, H. J. (2006). Welding characteristics on heat input changing of laser dissimilar metals welding. *Journal of Transactions of the Korean Society of Machine Tool Engineers, KSMTE, 15*(2), 51–58. **(in Korean)**.

Mun, J. M., Jeong, Y. S., Jeon, J. H., Ahn, J. H., & Kim, I. T. (2017). Experimentally evaluating fatigue behavior of corroded steels exposed in atmospheric environments. *Journal of Korean Society of Steel Construction, KSSC, 29*(3), 193–204. **(in Korean)**.

Park, J. E., Kyung, K. S., Moon, M. G., Koh, K. H., & Hong, Y. J. (2019). Experimental study on application of clean laser system in surface preparation on steel. *Journal of Korean Society of Steel Construction, KSSC, 31*(6), 447–458. **(in Korean)**.